Vegetable Research

ARTICLE

Open Access

https://doi.org/10.48130/vegres-0025-0015

Vegetable Research **2025**, 5: e019

Genome-wide identification, evolution and expression analysis of the *PP2C* gene family in ice plant

Di Guo[1#], Quanlong Liu[1#], Yuxuan Song[1#], Yani Cheng[1], Aojun Zhang[1], Yuhua Cui[1], Jiaqi Zhang[1], Wenbin Tong[1], Yusi Sun[1], Miaoyu Tian[1], Xinwei Li[1], Yingchao Zhang[1*] and Xiaoming Song[1,2,3,4*]

[1] *College of Life Sciences, North China University of Science and Technology, Tangshan 063210, China*
[2] *School of Basic Medical Sciences, North China University of Science and Technology, Tangshan 063210, China*
[3] *Hebei Key Laboratory of Medical Engineering and Integrated Utilization of Saline alkali Land, North China University of Science and Technology, Tangshan 063210, China*
[4] *Hebei Administration of TCM Key Laboratory of Quality Control of Salt alkali Resistant TCM, North China University of Science and Technology, Tangshan 063210, China*
[#] Authors contributed equally: Di Guo, Quanlong Liu, Yuxuan Song
[*] Corresponding authors, E-mail: zhangyc@ncst.edu.cn; songxm@ncst.edu.cn

Abstract

Potein phosphatase 2C (PP2C) plays essential roles in plant stress signal transduction. However, the *PP2C* gene family of ice plant (*Mesembryanthemum crystallinum*), halophytes that can grow under high salt conditions, has been rarely reported. Here, we conducted a genome-wide investigation of the *McrPP2C*s. A total of 59 *McrPP2C*s were identified. They were unevenly distributed across nine chromosomes and were divided into 12 clades (A–L). *McrPP2C* genes in the same clade had similar gene structures and conserved domains. Collinearity analysis showed that whole-genome duplication (WGD), particularly the proposed whole-genome triplication event (WGT), played a key role in the expansion of the ice plant *PP2C* gene family. *McrPP2C*s had experienced strong purifying selection pressure. 81.4% of *McrPP2C*s contained ABA-responsive elements (ABREs). Based on transcriptomic data, four clade A *McrPP2C*s (*McrPP2c11/15/17/35*) displayed significant up-regulation under salt treatments in leaf and root, indicating their essential roles in salt stress response. These results revealed the evolutionary trajectory of the ice plant *PP2C* gene family and indicated the potential roles of *McrPP2C*s under salt stress, which provides some clues for understanding why the ice plant has strong salt tolerance.

Citation: Guo D, Liu Q, Song Y, Cheng Y, Zhang A, et al. 2025. Genome-wide identification, evolution and expression analysis of the *PP2C* gene family in ice plant. *Vegetable Research* 5: e019 https://doi.org/10.48130/vegres-0025-0015

Introduction

As sessile organisms, plants have developed complex mechanisms in response to stress. Protein reversible phosphorylation is one of the most important regulatory strategies. Protein kinases phosphorylate serine (Ser), threonine (Thr), and tyrosine (Tyr), while protein phosphatases eliminate phosphate groups[1,2]. According to their substrate specificity, protein phosphatases can be divided into three categories: Ser/Thr phosphatases, phosphotyrosine phosphatase, and dual specificity phosphatases[2,3]. PP2C (Protein phosphatases 2C), the metal ion-dependent protein phosphatase, belongs to Ser/Thr phosphatases. PP2Cs, which merged early in evolution as distinct protein phosphatases, are the largest family of protein phosphatases, and are identified in archaea, bacteria, fungi, plants, and animals[4,5]. To date, *PP2C*s have been reported in many higher plants including *Arabidopsis* (80), rice (90), wheat (95), peanut (178), tomato (92), maize (102), cucumber (56), cotton (181 in *Gossypium hirsultum*, 87 in *Gossypium arboreum*, 147 in *Gossypium barbadense*, 99 in *Gossypium raimondii*), sweet cherry (76), *Rosa chinensis* Old Blush (69), soybean (126), quinoa (117), strawberry (56 in *Fragaria vesca*, 228 in *Fragaria ananassa*), etc[1,2,5–15]. *PP2C*s are highly conserved in evolution. They are divided into 13 clades (A–M) and some single branch members based on phylogenetic analysis[4,7]. Most of them have a conserved catalytic region at the C-terminus and a poorly conserved region at the N-terminus. The diversity of the N-terminus indicates that they have different functions in the signal transduction mechanism[1,2,4].

PP2Cs play vital roles in the plant response to abiotic environmental pressures[1,4]. Clade A PP2Cs participate in abscisic acid (ABA) signaling by physically interacting with SnRK2s, which inhibits activation of the downstream transcription factors[4,16–18]. When ABA accumulates, it binds to PYR1, which in turn binds to and inhibits PP2Cs. Then, the downstream SnRK2 kinases are released to active downstream target genes. Thus, clade A PP2Cs function as a switch of the ABA signaling network. This regulation often happens under osmotic stress conditions caused by drought and salinity[4,15–19]. However, transcription analysis demonstrates that many PP2Cs are up or down expressed under salt treatment, indicating other clades of PP2Cs are also involved in stress response[6,20]. Several PP2C B, and F repress the MAPK signal pathways activated by drought[4,21–23]. AtPP2C49 (G clade) represses AtHKT1.1 to regulate Na^+ distribution in *Arabidopsis* after salt treatment[24]. AtPP2C.D6 and D7 interact with SOS1 and inhibit its Na^+/H^+ antiporter activity in unstressed conditions. Under salt stress, SCaBP8 interacts with the PP2Cs suppresses their phosphatase activity, and simultaneously releases PP2C.D6 from the plasma membrane[25]. *AtPP2CG1* is fully expressed under salt stress and positively regulates salt tolerance in an ABA-dependent manner[26]. Over-expression of *ZmPP2C2* (clade B) in tobacco enhances cold stress tolerance by displaying higher germination speed and rate, higher antioxidant enzyme activities, and lower cold-induced electrolyte leakage and malondialdehyde contents[27]. A PP2C D clade gene, AtFGT2, affects the heat stress memory. *Fgt2* mutants are defective in the memory of heat stress[28]. Taken together, PP2Cs are important for plant abiotic stress responses.

Mesembryanthemum crystallinum (ice plant) is a halophyte that can grow under high salt conditions[29–32]. Mature ice plants are capable of growing in soil that contains 450 mM NaCl, which is

© The Author(s)

higher than the concentration found in seawater[29]. On MS medium, the root growth of ice plant continues in 140 mM NaCl, while the root growth of *Arabidopsis thaliana* is completely inhibited[29]. Moreover, ice plant switches from C3 photosynthesis to crassulacean acid metabolism (CAM) under high salinity stress, which is related to the key enzyme-phosphoenolpyruvate carboxylase (*McrPEPC*/08G01316) induction in leaf[30,31]. The C3-CAM switch allows ice plants to improve their salt tolerance by high efficiency of water use and CO_2 fixation[32]. In 2022, a high-quality ice plant genome sequence was reported, providing the data resource for comparative and functional genomic studies of ice plants on salt tolerance and C3-CAM transitions[31].

Since PP2Cs play crucial roles in plant stress response and ice plant can be adapt to extreme environments, we conducted a genome-wide investigation of the *PP2C* gene family in ice plant. In total, 59 *McrPP2C*s were identified and phylogenetic evolution, gene replication, selection pressure, and *cis*-regulatory elements were analyzed using bioinformatic methods. In addition, transcriptomic data was used to study *McrPP2C*s expression patterns under different NaCl treatments. The results will lay the foundation for understanding the potential roles of *McrPP2C*s under salt stress and why ice plant has a strong salt tolerance.

Materials and methods

Collection of genomic data and identification of the *PP2C* gene family

The data related to the *Arabidopsis thaliana* genome used in this study were sourced from the TAIR website (Tair10, www.arabidopsis.org). The genome and related data of *Mesembryanthemum crystallinum* were sourced from the database at NGDC (https://ngdc.cncb.ac.cn/). The data related to the genomes of *Vitis vinifera* and *Oryza sativa* were sourced from the JGI database (https://genome.jgi.doe.gov/portal/). The data related to the genomes of *Hylocereus undatus*, *Amaranthus caudatus*, and *Beta vulgaris* were sourced from the NCBI database (www.ncbi.nlm.nih.gov). The hmm file of the PP2C protein domain (PF00481) was downloaded from the Pfam database. Then, the whole genome of *M. crystallinum* and the five other species was identified using HMMER3.0[33] under the condition of an E-value of 1×10^{-5}. Through literature review, the sequence numbers of 80 PP2C genes of *A. thaliana* were obtained. The PP2C protein sequences of 80 *A. thaliana* were downloaded from the TAIR database (www.arabidopsis.org). The BLASTP[34] alignment was carried out between these sequences and the genome sequences of the other six plants at an E-value of 1×10^{-10}, and the members of the *PP2C* gene family (with a score > 100) were screened out. The genes obtained by taking the union of the sequences identified by HMMER3.0 and BLASTP were regarded as the preliminary members of the *PP2C* family. Finally, all the queryable databases were selected in the InterPro database[35], and the genes with the annotation of the keyword 'PP2C' were screened out as the final results.

Sequence analysis and basic information of the *PP2C* gene family

Wolf PSORT (WoLF PSORT: Protein Subcellular Localization Prediction) was used to predict the subcellular localization of PP2C proteins in *M. crystallinum* and six other plants. Expasy (SIB Swiss Institute of Bioinformatics | Expasy) was employed to analyze the molecular mass, instability coefficient, hydrophilicity, aliphatic index, and other parameters of the predicted PP2C proteins in *M. crystallinum* and the other plants.

Chromosomal localization of *PP2C* family members

Based on the genome annotation files, TBtools-II Gene Location Visualize from GTF/GFF module[36] was used to extract the chromosome length and the positional information of *PP2C* genes on the chromosomes from the genome annotation files of *M. crystallinum* and the other six plants. Then, TBtools-II was utilized to map the positions of PP2C genes on the chromosomes.

Construction of the phylogenetic tree of the *PP2C* gene family

The PP2C protein sequences of *M. crystallinum* and the other six species were subjected to multiple sequence alignment using Clustalw2 with its default parameters. Then, the Iqtree2 software[37] was employed to construct a phylogenetic tree. The Model-Finder Plus (MFP) method was used for the automatic estimation of the optimal substitution model, which turned out to be VT + R8. The bootstrap value was set to 1000, and other parameters were set to their default values.

Identification of collinearity and gene types in the *PP2C* gene family

Based on the BLASTP software, a homology search was conducted on the protein sequences of *M. crystallinum, H. undatus, A. caudatus, B. vulgaris, V. vinifera, A. thaliana,* and *O. sativa*. Then, the -icl module in WGDI was used to perform collinearity analysis[38]. The Advanced Circos in TBtools was utilized to visualize the collinearity results. Meanwhile, the Nei-Gojobori method in the -ks module of WGDI was employed to calculate the values of Ka, Ks, and Ka/Ks[39]. The duplicate_gene_classifier in MCScan[40] was used to count the number of different types of duplication events. Based on the neutral substitution rate 1.5×10^{-8} substitutions per site per year, the orthologous gene pairs were used for the divergence time estimation[41].

Analysis of the gene structure, conserved motifs, and *cis*-acting elements of the *PP2C* genes

Based on the coding sequences (CDS) and genomic DNA sequences of *PP2C*s, TBtools was used to draw the gene structure distribution maps. The conserved motif analysis of *PP2C*s was completed through the MEME online website, with the maximum number of motifs set to 10. Then, TBtools was employed to visualize the results. 2,000 bp upstream of the *PP2C*s start codon (ATG) were extracted as the promoter sequences. The PlantCARE database[42] was utilized to predict the *cis*-acting elements and their potential related functions, and home-make Python was used for visualization.

Plant growth conditions

Ice plant seeds were directly planted in soil (Klasmann-Deilmann 876) after imbibed at 4 °C for 2 d. Then the plants were grown at 23 ± 1 °C under 200 μmol·m^{-2}·s^{-1} white light with a 14 h/10 h day/night cycle. After about 6 weeks, the ice plants were irrigated with 500 mM NaCl once daily. After 36 h (short time) or 14 d (long time), the second pair of mature leaves were collected for RNA sequencing and qRT-PCR examination. Plants irrigated with water were used as a control.

Expression analysis

RNA sequencing data have been previously published[29–32] or from Prof Song research group at the North China University of Science and Technology. For qRT-PCR analysis, total RNA was isolated using RNA Easy Fast Plant Tissue Kit. First-strand cDNA was synthesized using the FastKing RT Kit (with gDNase). QRT-PCR was performed using SuperReal PreMix Plus (SYBR Green). All the above reagents were purchased from Tiangen, Tiangen Biotech (Beijing) Co., Ltd. One μL cDNA was used as a template. The qRT-PCR condition was two-step: ① 95 °C 15 min; ② 40 cycles of 95 °C 10 s, and

60 °C 30 s. *FNR1* was used as an internal control. Three replications were employed and the relative expression levels were calculated using the $2^{-\Delta\Delta C_T}$ method[1]. T-test was used to determine statistical differences (** $p < 0.01$, * $p < 0.05$). A p-value < 0.05 and absolute fold change ≥ 2.0 signified differential expression.

Results

Identification and analysis of the *PP2C* gene family

Since the ice plant is the only sequenced plant in the Aizoaceae family, to explore the evolution of *PP2C* genes, we selected several closely related species and model species, including *O. sativa*, *V. vinifera*, *A. caudatus*, *H. undatus*, *B. vulgaris,* and *A. thaliana*. A total of 59 *McrPP2C*s were identified from the genome of *M. crystallinum*, and 115, 86, 69, 87, 49, and 80 were identified in *O. sativa*, *V. vinifera*, *A. caudatus*, *H. undatus*, *B. vulgaris,* and *A. thaliana* respectively (Supplementary Tables S1–S8). The protein sequences of PP2Cs varied greatly. Their amino acid numbers ranged from 78 to 1,832. The isoelectric points were between 3.75 and 11.86. Most PP2Cs (420/545) were acidic proteins. The largest molecular mass was 206,639.9, and the smallest was 8,163.06. Among the 545 PP2Cs, stable proteins accounted for approximately 29.9% (163), and unstable proteins accounted for approximately 70.1% (382). The hydrophilicity of the proteins ranged from 0.274 to −1.248, and the aliphatic index was between 53.04 and 106.75. Subcellular localization predictions suggested that most PP2Cs may be located in the nucleus, chloroplast, or cytoplasm (Supplementary Tables S1–S7).

Chromosomal localization of the *PP2C* gene family

In *M. crystallinum*, 59 *McrPP2C*s were unevenly located on nine chromosomes (Fig. 1). Chr 3 had the largest number of *McrPP2C*s (11), while Chr 7 had the fewest *McrPP2C*s (3). Most *McrPP2C*s were concentrated near the two ends of each chromosome while fewer genes were in the centromeric regions. There was no positive correlation between the length of a chromosome and the number of *McrPP2C*s (Fig. 1; Supplementary Table S1). The distribution pattern of *PP2C*s in other six studied plants was similar (Supplementary Tables S2–S8).

Phylogenetic analysis of the *PP2C* gene family

To clarify the evolutionary relationships of *PP2C*s, the protein sequences of PP2Cs from the seven studied species were combined to construct a phylogenetic tree. According to the topological structure, 56 *McrPP2C*s were divided into 12 clades (A–L), and three *McrPP2C*s not assigned to any clade (Fig. 2, Table 1). Clade F had the largest number (9), followed by clade A (7). For the *PP2C*s of the other six studied species, the clades E or F were the largest in most cases. The only exception was *O. sativa*, in which clade D had the largest number (Fig. 2, Table 1). Each clade contained *PP2C*s from all seven species and genes from the same species tended to cluster together (Fig. 2, Table 1).

Amplification analysis of the *PP2C* gene family

Gene duplication promotes the expansion of gene families. We used MCScan to classify the gene types and divided all *PP2C*s into five groups: singletons, dispersed genes, proximal duplicates, tandem duplicates, and polyploidy-related genes (Table 2). WGD contributed most to gene expansion in *M. crystallinum* (76.3%), *V. vinifera* (75.6%), and *O. sativa* (48.2%). In contrast, dispersed duplications contributed most to gene expansion in *A. thaliana* (51.3%), *B. vulgaris* (69.4%), and *A. caudatus* (52.2%). In *H. undatus*, the proportions of dispersed genes and WGD were the same, indicating their same contributions to gene expansion. Singletons of PP2Cs were not detected among these seven species (Table 2).

Collinearity and selection pressure analysis of the *PP2C* gene family

To investigate the evolutionary relationships of *PP2C*s among different species, collinearity analysis was performed between *M. crystallinum* and the other six studied species to search for orthologous genes (Fig. 3a). The results showed that there were 80 pairs of orthologous genes between *M. crystallinum* and *H. undatus*, 95 pairs between *H. undatus* and *A. caudatus*, 57 pairs between *A. caudatus* and *B. vulgaris*, 55 pairs between *B. vulgaris* and *V. vinifera*, 80 pairs between *V. vinifera* and *A. thaliana*, and 23 pairs between *A. thaliana* and *O. sativa* (Supplementary Table S9). To explore the evolutionary patterns of *McrPP2C*s, collinearity analysis was also used to search for paralogous genes. Six gene pairs were identified in the 59 *McrPP2C*s, named as *McrPP2C2*/*McrPP2C4*, *McrPP2C11*/*McrPP2C12*, *McrPP2C15*/*McrPP2C23*, *McrPP2C19*/*McrPP2C29*, *McrPP2C47*/*McrPP2C51*, and *McrPP2C55*/*McrPP2C56*. The collinear genes were distributed on seven of nine chromosomes, except Chr4 and Chr6 (Fig. 3b). The divergence time between the six pairs of duplicated genes was calculated based on the mutation rate of 1.5×10^{-8} mutations per synonymous site per year (Supplementary Table S10). It was estimated that the divergence events occurred around 113.9–168.8 million years ago (Mya), very close to the whole-genome triplication event (WGT, 130–150 Mya).

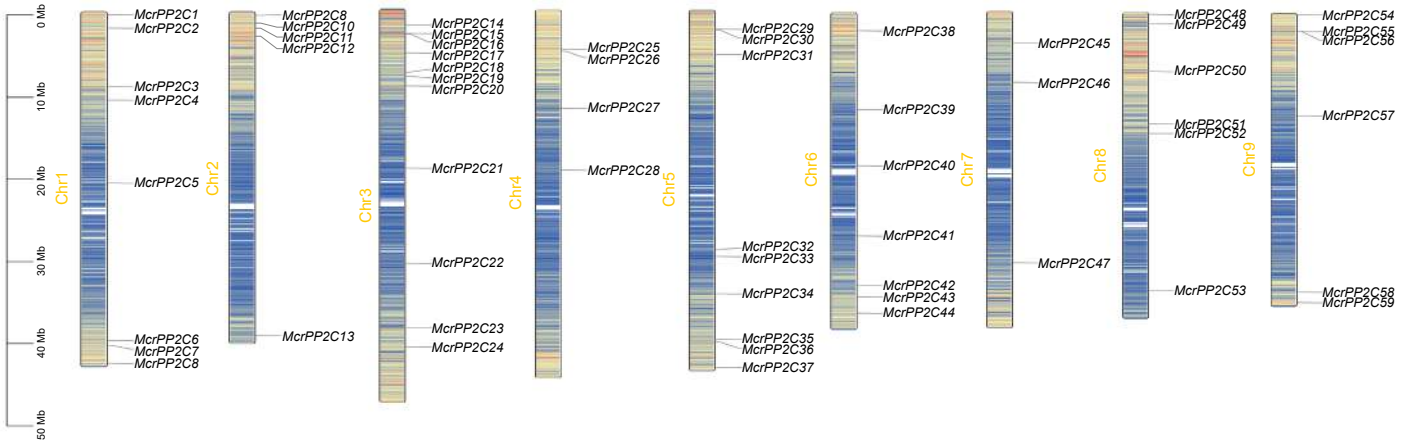


Fig. 1 Chromosome distribution of the *PP2C* gene family in *M. crystallinum*. *McrPP2C*s are marked on nine chromosomes and the chromosome length is demonstrated in the left scale. Different chromosomal colors indicate different gene densities, with red representing the highest density and blue representing the lowest density.

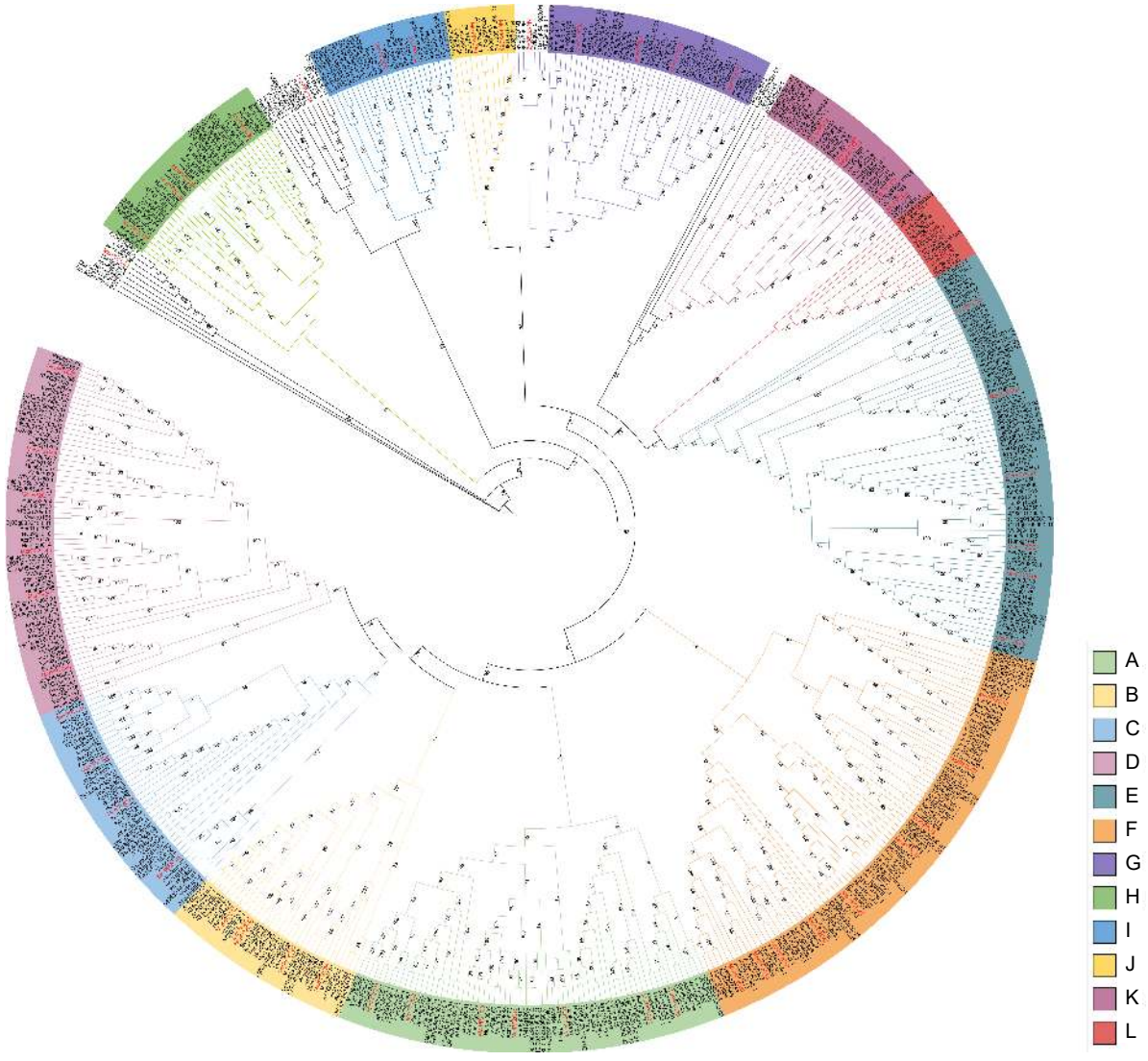


Fig. 2 Phylogenetic analysis of the *PP2C* gene family from *M. crystallinum*, *H. undatus*, *A. caudatus*, *B. vulgaris*, *V. vinifera*, *A. thaliana*, and *O. sativa*. Phylogenetic trees were constructed using the PP2C protein sequences and different colors indicate different clades. *PP2C* genes in *M. crystallinum* are marked in red.

Table 1. The number of *PP2C*s in each clade.

Clade	*O. sativa*	*V. vinifera*	*H. undatus*	*B. vulgaris*	*A. cruentus*	*A. thaliana*	*M. crystallinum*
A	13	12	10	6	9	9	7
B	4	4	6	4	4	6	5
C	8	6	6	3	7	7	5
D	17	9	11	4	8	9	6
E	15	7	13	9	10	12	6
F	12	17	13	8	11	12	9
G	8	6	6	4	5	6	4
H	9	5	5	3	5	3	2
I	12	2	2	2	2	2	3
J	2	2	2	1	1	2	2
K	7	9	4	1	2	3	5
L	2	2	2	1	2	2	2
Single Branch	6	4	6	3	3	7	3

To further study the divergence and selection in the gene duplication of *PP2C*s, the Ka/Ks values of the paralogous gene pairs in *M. crystallinum* were evaluated (Supplementary Table S11). The Ka/Ks values of all paralogous gene pairs in *M. crystallinum* and in the other six studied species were less than 1, demonstrating that these genes were mainly under purifying selection during the evolutionary process.

Analysis of the gene structure and conserved motifs of the *PP2C* gene family

Since the diversity of exon/intron structures plays an important role in the evolution of gene families, we analyzed the exon/intron structural patterns of *McrPP2C*s based on their phylogenetic relationships. The number of exons in *McrPP2C*s ranged from 2 to 19, and most members of the same clade possessed similar numbers of exons/introns with varied total gene lengths (Fig. 4). For instance, all clade A *McrPP2C*s have either three or four exons, but *McrPP2C17* was over 10 kb, more than 2 fold than other clade A members. The variation of gene length was mainly due to the different lengths of introns, while the length of exons was similar (Fig. 4), indicating that *McrPP2C*s are relatively conserved during the evolutionary process, thus resulting in similar functions.

To identify the common motifs in *McrPP2C*s, we utilized the MEME motif search tool to determine 10 conserved motifs[2]. The number of motifs contained in *McrPP2C*s ranges from 3 to 10. Some motifs exhibited a certain degree of conservation. Motif 3 could be found

Table 2. The identification of duplicated types for *PP2C* genes and all genes in ice plant.

	Species	Singleton		Dispersed		Proximal		Tandem		WGD or segmental		Total
PP2Cs	*M. crystallinum*	0	0	11	18.6%	1	1.7%	2	3.4%	45	76.3%	59
	H. undatus	0	0	38	44.2%	7	8.1%	3	3.5%	38	44.2%	86
	A. cruentus	0	0	36	52.2%	4	5.8%	3	4.3%	26	37.7%	69
	B. vulgaris	0	0	34	69.4%	4	8.2%	6	12.2%	5	10.2%	49
	V. vinifera	0	0	15	17.4%	1	1.2%	5	5.8%	65	75.6%	86
	A. thaliana	0	0	41	51.3%	0	0.0%	3	3.8%	36	45.0%	80
	O. sativa	0	0	34	40.0%	6	7.1%	4	4.7%	41	48.2%	85
Whole genome	*M. crystallinum*	4,008	17.3%	6,915	29.8%	979	4.2%	2,527	10.9%	8,754	37.8%	23,183
	H. undatus	4,798	17.5%	9,867	35.9%	1,638	6.0%	2,836	10.3%	8,351	30.4%	27,490
	A. cruentus	5,963	23.9%	10,958	43.9%	845	3.4%	2,010	8.0%	5,210	20.9%	24,986
	B. vulgaris	7,247	32.4%	10,780	48.1%	1,308	5.8%	2,148	9.6%	908	4.1%	22,391
	V. vinifera	4,906	14.4%	10,025	29.4%	2,359	6.9%	4,628	13.6%	12,152	35.7%	34,070
	A. thaliana	5,590	20.4%	9,861	35.9%	1,061	3.9%	3,126	11.4%	7,807	28.4%	27,445
	O. sativa	12,761	33.9%	13,402	35.6%	2,627	7.0%	2,982	7.9%	5,858	15.6%	37,630

in all *McrPP2Cs*; motif 1 did not exist only in *McrPP2C53*; motif 6 did not existed in *McrPP2C22* and *McrPP2C39* (Fig. 4; Supplementary Table S12). *McrPP2Cs* in the same branch had similar distribution orders and numbers of motifs (Fig. 4; Supplementary Table S12).

Prediction of *cis*-acting elements of the *PP2C* gene family

To further clarify the potential functions of *McrPP2Cs*, the *cis*-acting elements in the 2-kb upstream regions were analyzed. The results showed that *McrPP2Cs* contained four types of *cis*-acting elements: light-responsive elements, hormone-responsive elements, defense and stress-responsive elements, and growth and development-related elements (Fig. 5; Supplemental Table S13). Among them, light-responsive elements were present in all *McrPP2Cs* and were the most abundant in number, suggesting that *McrPP2Cs* are closely related to light regulation in *M. crystallinum*. The hormone responsive elements of *McrPP2Cs* included abscisic acid (ABA)-responsive elements, gibberellin-responsive elements, and methyl jasmonate (MeJA)-responsive elements. Among them, ABA-responsive elements existed in most *McrPP2Cs*. Only 11 of 59 *McrPP2Cs* did not contain ABA-responsive elements. *McrPP2C2* and *McrPP2C11* had the largest number of ABA-responsive elements. Besides, most *McrPP2Cs* contained MeJA-responsive elements. *McrPP2C11* had the largest number (12). The environmental pressure response elements of *McrPP2Cs* consisted of low temperature, drought, anaerobic induction, and stress response elements. Most *McrPP2Cs* contained anaerobic induction elements and more than half *McrPP2Cs* contained drought induction elements. In addition, the promoters of *McrPP2Cs* genes also contained elements related to plant growth and development (Fig. 5; Supplementary Table S13). These results suggested that *McrPP2Cs* may be widely involved in the stress response, as well as in plant growth and development.

Expression profiling of *McrPP2Cs* under salt stress

Ice plant can grow under high concentrations of NaCl[29–32]. One reason is that it can shift from C3 to CAM under salt stress[30–32]. Since this transition is related to the *McrPEPC*/08G01316 induction in leaf[29–32], we examined the expression profiling of *McrPP2Cs* under salt stress before and after the *McrPEPC* was induced. According to previous studies, we selected 14 d as a long time salt treatment, under which *McrPEPC* is fully induced[32]; and we selected 36 h as a short time salt treatment, under which *McrPEPC* cannot be induced[30]. Transcriptomic data confirmed that only long time salt treatment induced McrPEPC/Mc08G01316 (Supplementary Table S14). However, the expression changes of *McrPP2Cs* were similar under both long and short time treatments. Compared with the control, only four *McrPP2Cs* (*McrPP2c11*/Mc02G00242, *McrPP2c15*/Mc03G00348, *McrPP2c17*/Mc03G00607, *McrPP2c35*/Mc05G02416) were up-regulated after both long and short time salt treatments, while most *McrPP2Cs* did not show significant changes (Fig. 6a, b; Supplementary Tables S15, S16). Interestingly, all four up-regulated genes belonged to clade A. QRT-PCR was used to explore the expression pattern of all seven clade A *McrPP2Cs* and the results were consistent with the RNA-seq data (Fig. 6e).

To better understand the expression pattern of clade A *McrPP2Cs* under salt stress, we reanalyzed the published RNA-seq data in root[29,31]. In root, six clade A *McrPP2Cs* were induced under 500 mM NaCl treatment except *McrPP2C34*/Mc05G01962 (Fig. 6c; Supplementary Table S17). We also explored the expression of clade A *McrPP2Cs* in vegetable tissues using published data[31,42]. We found that all clade A *McrPP2Cs* expressed higher in root than in leaf, although their expression level varied (Fig. 6d; Supplementary Table S18). The expression level of *McrPP2C2*/Mc01G00236 was much higher than the other six *McrPP2Cs* in both leaf and root (Fig. 6d; Supplementary Table S18). Primers are shown in Supplementary Table S19.

Discussion

PP2Cs are widely identified in plants and play important roles in abiotic stress[1–5]. This study provides the first comprehensive analysis of the *PP2C* gene family in ice plants at the whole genome level. Finally, 59 *McrPP2Cs* were identified and most of them were clustered at the ends of chromosomes (Fig. 1; Supplementary Table S1). This uneven distribution might be because more repetitive sequences exist in the centromere than the ends. Similar distributions were also found in in the other six studied and some reported plants, including *Arabidopsis*, rice, wheat, peanut, cucumber, strawberries, tomato, soybean, sweet cherry, etc (Supplementary Table S8)[1,2,6–15], suggesting the genes uneven distribution is prevalent in higher plants. This phenomenon indicated that the recombination active chromosome arms tend to retain stress-responsive genes, while the centromere regions enriched in repetitive sequences showed selective limitation of gene retention. Phylogenetic analysis divided the *McrPP2Cs* into 12 clades (A-L) and genes from the same species tended to cluster together (Fig. 2). This means PP2Cs retain their core functions while undergoing differentiation at the species level, which may be driven by adaptation to unique environmental challenges. In addition, most of the genes on the same chromosome did not belong to the same subfamily in the phylogenetic tree (Figs 1, 2), suggesting that genes on the same chromosome perform different functions.

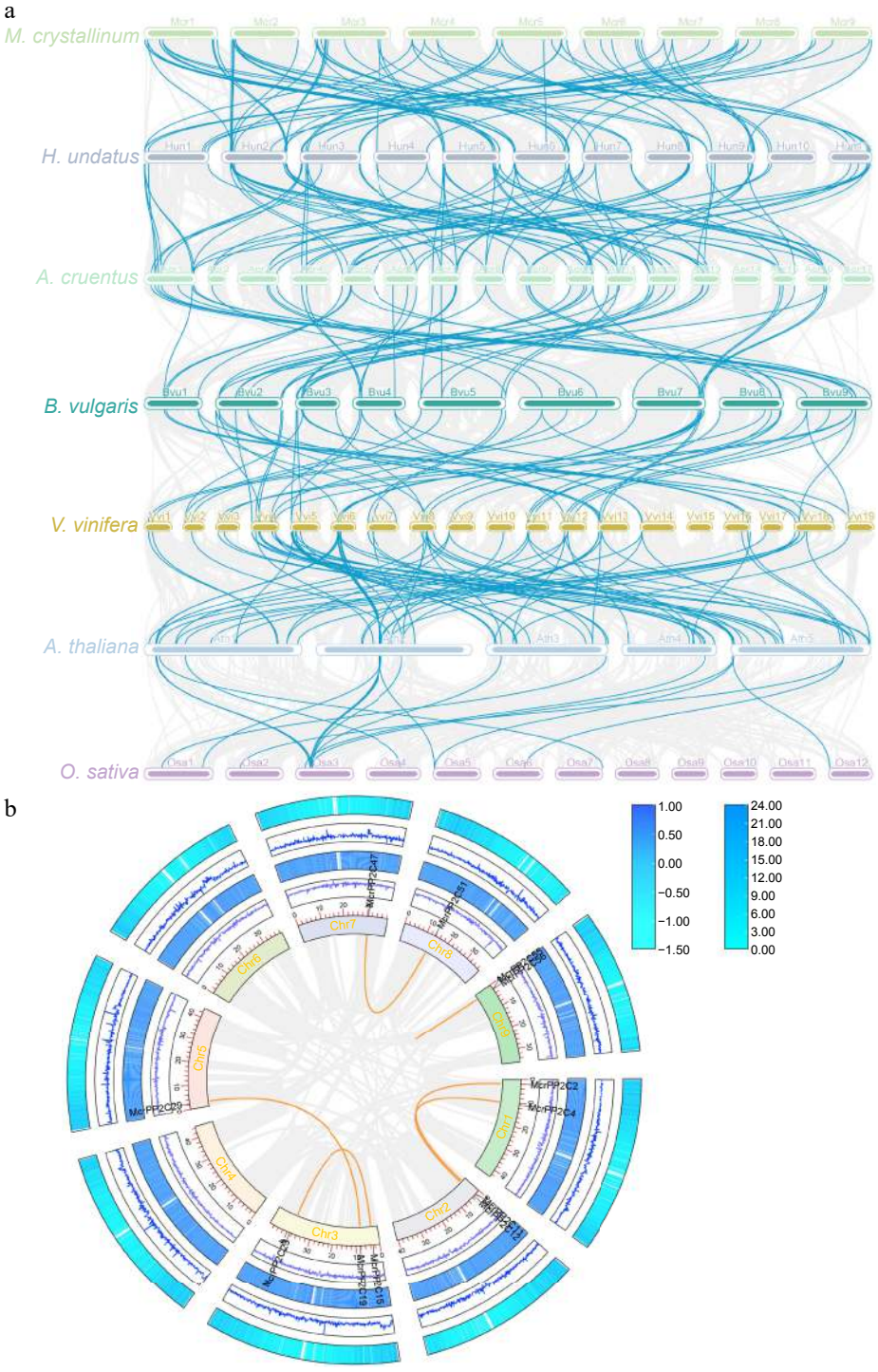


Fig. 3 Collinearity analysis of the *PP2C* gene family. (a) The collinear genes are shown by gray lines, while the syntenic *PP2C* homologous gene pairs are highlighted by blue lines. The species from top to bottom are *M. crystallinum*, *H. undatus*, *A. caudatus*, *B. vulgaris*, *V. vinifera*, *A. thaliana*, and *O. sativa*. (b) Collinearity analysis of *McrPP2C*s. The gray lines represent all collinear genes in the ice plant, and orange lines represent the *McrPP2C* collinearity genes.

In ice plants, the largest *McrPP2C* clade was F, which had nine genes (Fig. 2, Table 1). This clade is also the largest in many other plants such as *Arabidopsis*, grape, wheat, *B. vulgaris*, *H. undatus*, etc (Fig. 2, Table 1)[7]. It is reported that clade F *PP2C* negatively regulates stomata closure under drought stress in maize[22]. Thus, we speculated that plants developed redundant clade F *PP2C*s to regulate the stomata movement during stress responses. Since ice plant converts from C3 photosynthesis to CAM under high salinity stress, the stomata convert from a night-closure to a night-opening pattern[30,31]. Therefore, the large clade F *McrPP2C*s may be involved in this stomata conversion. However, the expression pattern of clade F *McrPP2C*s was not changed after salt treatment in leaf (Fig. 6a, b; Supplementary Tables S15, S16), implying that there was post-transcriptional regulation on clade F *McrPP2C*s.

In plants, gene duplication promotes the expansion of gene families. Whole-genome duplication (WGD) contributed the most to the expansion of *PP2C*s family in *M. crystallinum, V. vinifera,* and *O. sativa* (Table 2). Our previous study shows that *M. crystallinum* has only

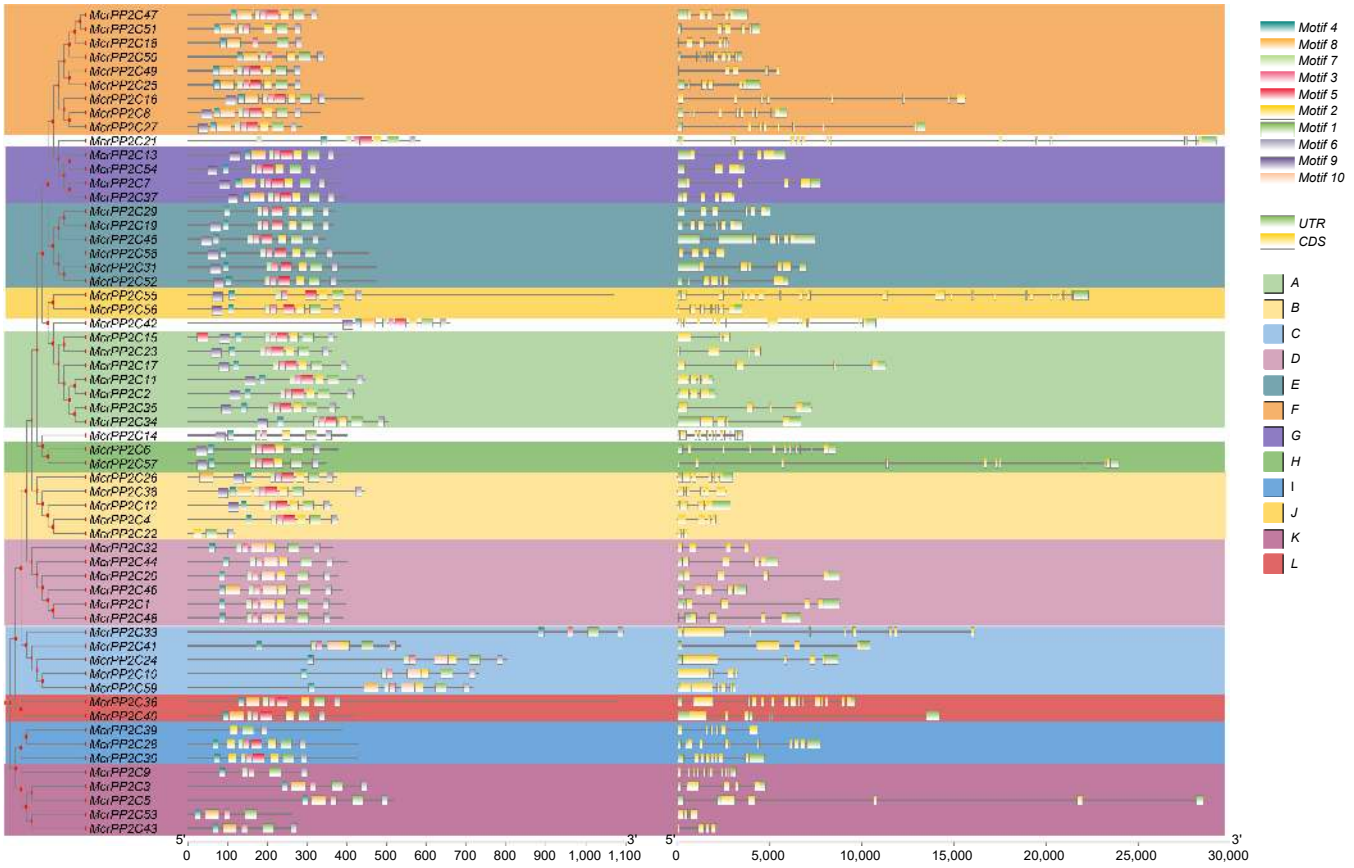


Fig. 4 The motif and exon-intron structure analyses of the *PP2C* gene family in *M. crystallinum*.

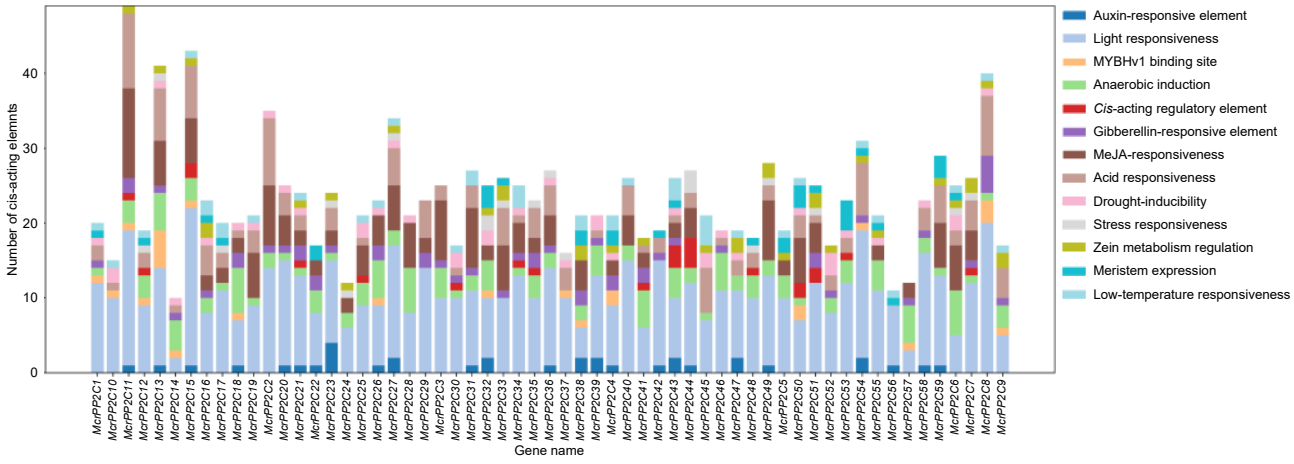


Fig. 5 *Cis*-elements analysis of *PP2C* genes in *M. crystallinum*. Different colors indicate different components. The vertical bar indicate the number of elements.

experienced one whole-genome triplication (WGT) event[31]. The differentiation time (113.9–168.8 Mya) of six pairs of paralogous *McrPP2C*s was highly consistent with their WGT events (approximately 130–150 Mya), strongly supporting that WGT was a key driving force for PP2C family expansion (Table 2). Because WGD events are often accompanied by large-scale gene loss and gene recombination[43], the number of *McrPP2C*s may be underestimated. However, compared with the 23,183 annotated genes in *M. crystallinum*, the 59 *McrPP2C*s retention is still extremely significantly higher than expected by chance (Chi-square test *p*-value = 8.22446E-06 < 0.05) (Table 2)[44], suggesting the strong selection pressure towards retaining these genes, which may be attributed to the strong stress tolerance in ice plant. In contrast, the expansion of the *PP2C* family in *A. thaliana* and *B. vulgaris* is mainly through dispersed replication, reflecting the differences in evolutionary strategies of species with different polyploidization histories.

Collinearity analysis and a previous study demonstrated that 46.3% of the orthologous genes between *M. crystallinum* and *H. undatus* appeared before the species divergence (~77.8 Mya)[31], indicating that the *PP2C* family existed in the common ancestor of *M. crystallinum* and *H. undatus* and had already formed a certain evolutionary basis before species differentiation. Two up-regulated clade A *McrPP2C*s (*McrPP2C11*/Mc02G00242, *McrPP2C15*/*Mc03G00348*) had colinear genes, *McrPP2C12*/Mc02G00368 and

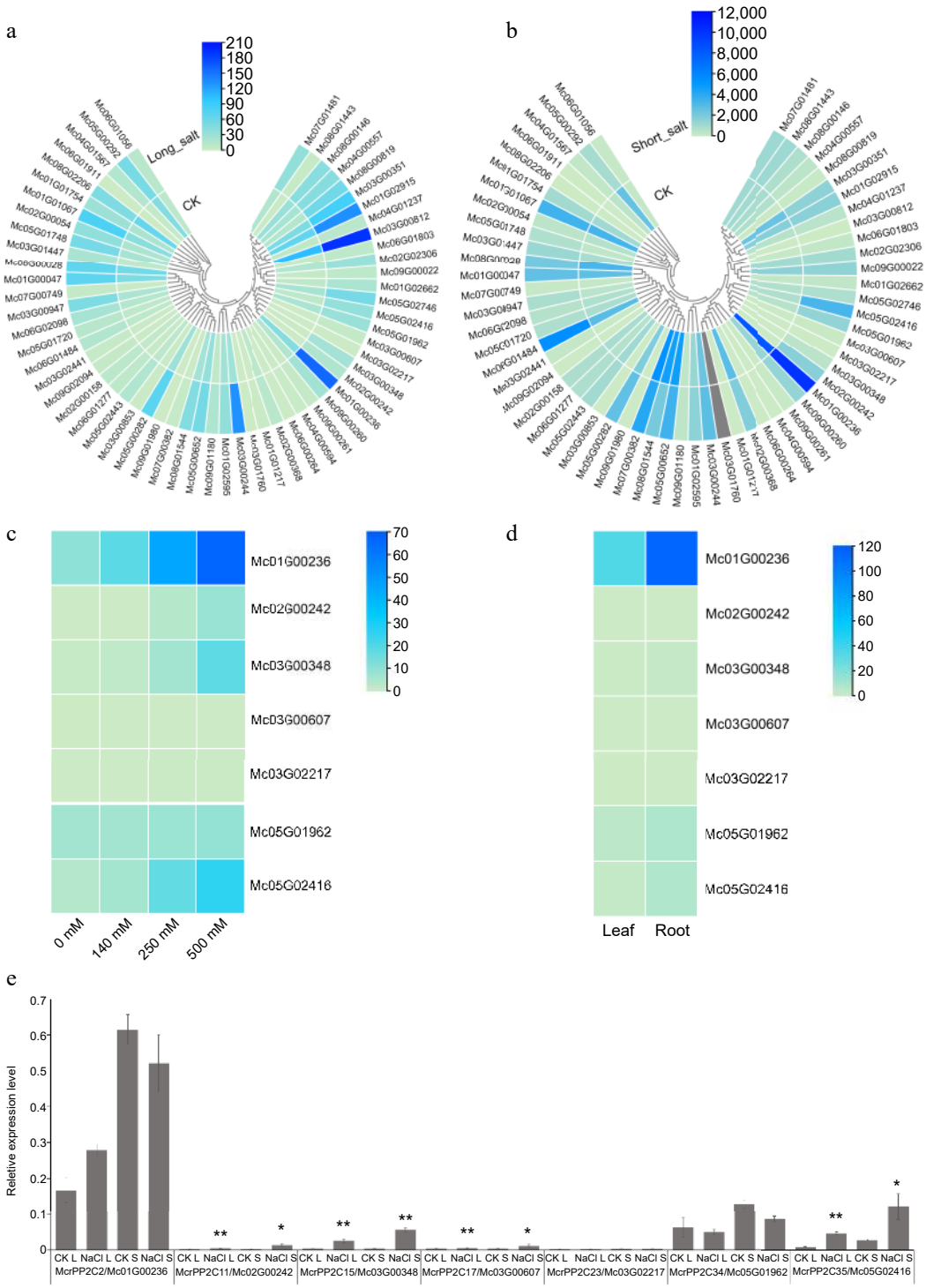


Fig. 6 Expression pattern analysis of *PP2C* genes in *M. crystallinum*. Expression pattern analysis of *McrPP2Cs* in leaf under (a) 14 d and (b) 36 h salt stress. CK indicates the corresponding control group. Grey bars mean the gene was not detected. (c) Expression pattern analysis of clade A *McrPP2Cs* in root under different NaCl treatments. (d) Expression pattern analysis of clade A *McrPP2Cs* in leaf and root under unstressed condition. (e) qRT-PCR analysis of clade A *McrPP2Cs* in leaf under long and short salt stress. CK L: 14 d salt stress control; NaCl L: 14 d salt stress; CK S: 36 h salt stress control; NaCl S: 36 h salt stress. Compared with corresponding control, a *p*-value < 0.05 and absolute fold change ≥ 2.0 signified differential expression (* $p < 0.05$, ** $p < 0.01$).

McrPP2C23/Mc03G2217 respectively (Fig. 3b). But expression level of the colinear genes were not changed under salt stress (Fig. 6a, b). This different expression pattern may be caused by subfunctionalization or neofunctionalization after gene duplication. The genome retains redundant genes to meet complex regulatory requirements. This dynamic evolutionary strategy may be an important mechanism for salt tolerance in ice plants. The Ka/Ks values of all *McrPP2C* paralogous gene pairs were far less than 1 (Supplementary Table S11), indicating that they were subjected to purify selection, which might help maintain the basic functions of *PP2C* genes.

Gene structure and expression analysis found that differences in exon-intron structure and motif composition were not related to the expression pattern. For example, there was one more exon in *McrPP2C15*/*Mc03G00348* compared with other clade A *McrPP2Cs*,

but its expression pattern was similar to the other three clade A *McrPP2Cs* (*McrPP2C11*/Mc02G00242, *McrPP2C17*/Mc03G00607, *McrPP2C35*/Mc05G02416) in leaf and root under salt stress (Figs 4, 6). Promoter analysis showed that *McrPP2Cs* were rich in light-responsive, hormone-responsive, and drought-responsive elements. 81.4% of *McrPP2Cs* contained ABA-responsive elements (ABREs) (Fig. 5; Supplementary Table S13). This is consistent with their stress responsive functions. Besides, MeJA responsive elements were also widely spread in *McrPP2Cs* promoter (Fig. 5; Supplementary Table S13). In *Arabidopsis*, JA level is elevated in response to mites and necrotrophic pathogens[45]. Therefore, *McrPP2Cs* may be the cross-linking of biotic and abiotic stress signals. It is worth noting that *McrPP2C2*/Mc01G01236 and *McrPP2C11*/Mc02G00242 owned the highest number of ABREs, 9 and 10 respectively (Fig. 5; Supplementary Table S13). Both of them belong to clade A *McrPP2Cs*. Since this clade is tightly related to ABA signal[4], these two genes might be key regulatory factors in the ABA dependent pathway. *McrPP2C11* could be induced in leaf and root by NaCl, whereas *McrPP2C2* was only induced by NaCl in root (Fig. 6a–c). This may be because the expression level of *McrPP2C2* was significantly higher in root compared with that in leaf (Fig. 6d). In addition, the expression level of *McrPP2C2* was much higher than the other six clade A *McrPP2Cs* in both leaf and root (Fig. 6d) indicating it may play other roles besides ABA-dependent salt stress response in ice plants.

In our study, more than half clade A *McrPP2Cs* were up-regulated under salt stress (Fig. 6; Supplementary Tables S15–S18). *McrPP2C11*, *15*, *17*, *35* were induced in both leaf and root. *McrPP2C2*, *23* were only induced in root. The reason that more clade A *McrPP2Cs* were induced in root may be because the root directly contacts with the salinity. Under salt stress, ice plant shifts from C3 photosynthesis to CAM, which is related to the key enzyme *McrPEPC*/Mc08G01316 induction[30,31,42]. Our results showed that four clade A *McrPP2Cs* were induced earlier than *McrPEPC* in leaf, and the induction could be maintained for a long time (Fig. 6e; Supplementary Table S14). The quick response of *McrPP2Cs* suggested they may be involved in *McrPEPC* induction. Since clade A PP2Cs participate in the ABA signaling pathway, we believe that the ABA signal plays a central role in the C3-CAM transition. But the detailed molecular mechanism is unclear and needs to be further investigated.

Conclusions

In this study, we conducted a genome-wide identification and analysis of the *PP2Cs* in ice plants. A total of 59 *McrPP2Cs* were identified which were unevenly distributed across nine chromosomes with clustering near chromosome ends. Phylogenetic analysis classified *PP2Cs* of seven plant species into 12 clades (A–L), with *McrPP2Cs* distributed across all clades. A whole-genome triplication event (WGT, ~130–150 Mya) was identified as the primary driver of *McrPP2C* expansion, with 76.3% of gene duplication events attributed to WGT. Purifying selection dominates paralogue evolution. By predicting the *cis*-elements in the promoter, we found that 81.4% of *McrPP2Cs* contained ABA-responsive elements (ABREs). Under salt treatments, four clade A *McrPP2Cs* (*McrPP2c11*/*15*/*17*/*35*) displayed significant up-regulation in leaf and root, while two clade A *McrPP2Cs* (*McrPP2c2*/23) were only up-regulated in root. These results provide further insights into the ice plant *PP2C* gene family and indicate that they are potentially involved in the response to salt stress, which gives some clues for understanding why ice plant has strong salt tolerance.

Author contributions

The authors confirm contribution to the paper as follows: experiments design and performing: Guo D, Liu Q, Song Y; data collection and bioinformatics analysis: Guo D, Liu Q, Cheng Y, Zhang A, Cui Y, Zhang J, Tong W, Sun Y, Tian M, Li X; RNA extraction and qRT-PCR performing: Guo D, Song Y; manuscript preparation and revision: Guo D, Liu Q, Song Y, Song X, Zhang Y. All authors reviewed the results and approved the final version of the manuscript.

Data availability

All data generated or analyzed in this study are included in this published article and the supplemental files.

Acknowledgments

This work was supported by the College Students' Innovative Entrepreneurial Training Plan Program (S202410081037 and SK202403), the Basic Research Funds for Provincial Universities Basic Research Projects of North China University of Science and Technology (JQN2023036), Tangshan Science and Technology Plan Project (24130219C), the Basic research expenses for provincial universities (JJC2024001), the Natural Science Foundation for Distinguished Young Scholars of Hebei (C2022209010), the S&T Program of Hebei (23372505D), and the Hebei Natural Science Foundation (H2023209084).

Conflict of interest

The authors declare that they have no conflict of interest.

Supplementary information accompanies this paper at (https://www.maxapress.com/article/doi/10.48130/vegres-0025-0015)

Dates

Received 2 March 2025; Revised 6 April 2025; Accepted 16 April 2025; Published online 10 June 2025

References

1. Wu Z, Luo L, Wan Y, Liu F. 2023. Genome-wide characterization of the *PP2C* gene family in peanut (*Arachis hypogaea* L.) and the identification of candidate genes involved in salinity-stress response. *Frontiers in Plant Science* 14:1093913
2. Zhang G, Zhang Z, Luo S, Li X, Lyu J, et al. 2022. Genome-wide identifcation and expression analysis of the cucumber *PP2C* gene family. *BMC Genomics* 23:563
3. Farkas I, Dombrádi V, Miskei M, Szabados L, Koncz C. 2007. *Arabidopsis* PPP family of serine/threonine phosphatases. *Trends in Plant Science* 12(4):169–76
4. Wang Y, Xu C, Li G, Ding Z, Zheng S. 2023. Research progress of protein phosphatases type 2C family in response to various stresses in plants. *Plant Physiology Journal* 59(8):1463–73
5. Fuchs S, Grill E, Meskiene I, Schweighofer A. 2013. Type 2C protein phosphatases in plants. *The FEBS Journal* 280:681–93
6. Xue T, Wang D, Zhang S, Ehlting J, Ni F, et al. 2008. Genome-wide and expression analysis of protein phosphatase 2C in rice and *Arabidopsis*. *BMC Genomics* 9:550
7. Yu X, Han J, Wang E, Xiao J, Hu R, et al. 2019. Genome-wide identification and homoeologous expression analysis of *PP2C* genes in wheat (*Triticum aestivum* L.). *Frontiers in Genetics* 10:561
8. Qiu J, Ni L, Xia X, Chen S, Zhang Y, et al. 2022. Genome-wide analysis of the protein phosphatase 2C genes in tomato. *Genes* 13(4):604

9. Pang Y, Cao L, Ye F, Ma C, Liang X, et al. 2024. Identification of the maize *PP2C* gene family and functional studies on the role of *ZmPP2C15* in drought tolerance. *Plants* 13:340
10. Shazadee H, Khan N, Wang J, Wang C, Zeng J, et al. 2019. Identification and expression profiling of protein phosphatases (*PP2C*) gene family in *Gossypium hirsutum* L. *International Journal of Molecular Sciences* 20:1395
11. Liu B, Zhang Q, Qi L, Wu Y, Wang Y. 2024. Genomic-wide identification and expression analysis of the PP2C gene family in sweet cherry. *Acta Agriculturae Zhejiangensis* 36(10):2204−18
12. Shen Y, Zou J, Luo P, Shang W, Li Y, et al. 2023. Genome-wide identification and abiotic stress response analysis of PP2C family genes in *Rosa chinensis* 'Old Blush'. *Acta Horticulturae Sinica* 50(10):2139−56
13. Yang X, Tang M, Zhang B. 2022. Identification of soybean PP2C family genes and transcriptome analysis in response to salt stress. *Acta Agriculturae Zhejiangensis* 34(2):207−20
14. Yang D. 2024. *Identification and functional analysis of PYL-PP2C-SnRK2s gene family in quinoa (Chenopodium quinoa Willd.)*. Thesis. Yantai University, China. pp. 43
15. Guo L, Lu S, Liu T, Nai G, Ren J, et al. 2023. Genome-wide identification and abiotic stress response analysis of PP2C gene family in woodland and pineapple strawberries. *International Journal of Molecular Sciences* 24(4):4049
16. Park SY, Fung P, Nishimura N, Jensen DR, Fujii H, et al. 2009. Abscisic acid inhibits type 2C protein phosphatases via the PYR/PYL family of START proteins. *Science* 324(5930):1068−71
17. de Zelicourt A, Colcombet J, Hirt H. 2016. The role of MAPK modules and ABA during abiotic stress signaling. *Trends in Plant Science* 21(8):677−85
18. Jung C, Nguyen NH, Cheong JJ. 2020. Transcriptional regulation of protein phosphatase 2C genes to modulate abscisic acid signaling. *International Journal of Molecular Sciences* 21:9517
19. Yoshida T, Mergner J, Yang Z, Liu J, Kuster B, et al. 2024. Integrating multi-omics data reveals energy and stress signaling activated by abscisic acid in *Arabidopsis*. *The Plant Journal* 119:1112−33
20. Sun BR, Fu CY, Fan ZL, Chen Y, Chen WF, et al. 2019. Genomic and transcriptomic analysis reveal molecular basis of salinity tolerance in a novel strong salt-tolerant rice Landrace Changmaogu. *Rice* 12:99
21. Smékalová V, Doskočilová A, Komis G, Šamaj J. 2014. Crosstalk between secondary messengers, hormones and MAPK modules during abiotic stress signalling in plants. *Biotechnology Advances* 32(1):2−11
22. Brock AK, Willmann R, Kolb D, Grefen L, Lajunen HM, et al. 2010. The *Arabidopsis* mitogen-activated protein kinase phosphatase *PP2C5* affects seed germination, stomatal aperture, and abscisic acid-inducible gene expression. *Plant Physiology* 153(3):1098−111
23. Zhang P, Yuan Z, Wei L, Qiu X, Wang G, et al. 2022. Overexpression of *ZmPP2C55* positively enhances tolerance to drought stress in transgenic maize plants. *Plant Science* 314:111127
24. Chu M, Chen P, Meng S, Xu P, Lan W. 2021. The *Arabidopsis phosphatase* PP2C49 negatively regulates salt tolerance through inhibition of AtHKT1;1. *Journal of Integrative Plant Biology* 63(3):528−42
25. Fu H, Yu X, Jiang Y, Wang Y, Yang Y, et al. 2023. SALT OVERLY SENSITIVE 1 is inhibited by clade D Protein phosphatase 2C D6 and D7 in *Arabidopsis thaliana*. *The Plant Cell* 35:279−97
26. Liu YY, Shi WS, Liu Y, Gao XM, Hu B, et al. 2022. MdPP2C24/37, protein phosphatase type 2Cs from apple, interact with MdPYL2/12 to negatively regulate ABA signaling in transgenic *Arabidopsis*. *International Journal of Molecular Sciences* 23:14375
27. Hu X, Liu L, Xiao B, Li D, Xing X, et al. 2010. Enhanced tolerance to low temperature in tobacco by over-expression of a new maize protein phosphatase 2C, ZmPP2C2. *Journal of Plant Physiology* 167(15):1307−15
28. Urrea Castellanos R, Friedrich T, Petrovic N, Altmann S, Brzezinka K, et al. 2020. FORGETTER2 protein phosphatase and phospholipase D modulate heat stress memory in *Arabidopsis*. *The Plant Journal* 104:7−17
29. Tsukagoshi H, Suzuki T, Nishikawa K, Agarie S, Ishiguro S, et al. 2015. RNA-seq analysis of the response of the halophyte, *Mesembryanthemum crystallinum* (ice plant) to high salinity. *PLoS One* 10(2):e0118339
30. Kong W, Yoo MJ, Zhu D, Noble JD, Kelley TM, et al. 2020. Molecular changes in *Mesembryanthemum crystallinum* guard cells underlying the C3 to CAM transition. *Plant Molecular Biology* 103(6):653−67
31. Shen S, Li N, Wang Y, Zhou R, Sun P, et al. 2022. High-quality ice plant reference genome analysis provides insights into genome evolution and allows exploration of genes involved in the transition from C3 to CAM pathways. *Plant Biotechnology Journal* 20(11):2107−22
32. Cushman JC, Tillett RL, Wood JA, Branco JM, Schlauch KA. 2008. Large-scale mRNA expression profiling in the common ice plant, *Mesembryanthemum crystallinum*, performing C3 photosynthesis and Crassulacean acid metabolism (CAM). *Journal of Experimental Botany* 59(7):1875−94
33. Potter SC, Luciani A, Eddy SR, Park Y, Lopez R, et al. 2018. HMMER web server: 2018 update. *Nucleic Acids Research* 46(W1):W200−W204
34. Camacho C, Coulouris G, Avagyan V, Ma N, Papadopoulos J, et al. 2009. BLAST+: architecture and applications. *BMC Bioinformatics* 10:421
35. Jones P, Binns D, Chang HY, Fraser M, Li W, et al. 2014. InterProScan 5: genome-scale protein function classification. *Bioinformatics* 30:1236−40
36. Chen C, Wu Y, Li J, Wang X, Zeng Z, et al. 2023. TBtools-II: a "one for all, all for one" bioinformatics platform for biological big-data mining. *Molecular Plant* 16(11):1733−42
37. Minh BQ, Schmidt HA, Chernomor O, Schrempf D, Woodhams MD, et al. 2020. Corrigendum to: IQ-TREE 2: new models and efficient methods for phylogenetic inference in the genomic era. *Molecular Biology and Evolution* 37(8):2461
38. Sun P, Jiao B, Yang Y, Shan L, Li T, et al. 2022. WGDI: a user-friendly toolkit for evolutionary analyses of whole-genome duplications and ancestral karyotypes. *Molecular Plant* 15(12):1841−51
39. Wang T, Hu J, Ma X, Li C, Yang Q, et al. 2020. Identification, evolution and expression analyses of whole genome-wide TLP gene family in *Brassica napus*. *BMC Genomics* 21(1):264
40. Wang Y, Tang H, Wang X, Sun Y, Joseph PV, et al. 2024. Detection of colinear blocks and synteny and evolutionary analyses based on utilization of MCScanX. *Nature Protocols* 19(7):2206−29
41. Song X, Sun P, Yuan J, Gong K, Li N, et al. 2021. The celery genome sequence reveals sequential paleo-polyploidizations, karyotype evolution and resistance gene reduction in Apiales. *Plant Biotechnology Journal* 19(4):731−44
42. Lescot M, Déhais P, Thijs G, Marchal K, Moreau Y, et al. 2002. PlantCARE, a database of plant *cis*-acting regulatory elements and a portal to tools for in silico analysis of promoter sequences. *Nucleic Acids Research* 30(1):325−27
43. Freeling M, Woodhouse MR, Subramaniam S, Turco G, Lisch D, et al. 2012. Fractionation mutagenesis and similar consequences of mechanisms removing dispensable or less-expressed DNA in plants. *Current Opinion in Plant Biology* 15(2):131−39
44. Song XM, Wang JP, Sun PC, Ma X, Yang QH, et al. 2020. Preferential gene retention increases the robustness of cold regulation in *Brassicaceae* and other plants after polyploidization. *Horticulture Research* 7:20
45. Schweighofer A, Kazanaviciute V, Scheikl E, Teige M, Doczi R, et al. 2007. The PP2C-type phosphatase AP2C1, which negatively regulates MPK4 and MPK6, modulates innate immunity, jasmonic acid, and ethylene levels in *Arabidopsis*. *The Plant Cell* 19:2213−24

Copyright: © 2025 by the author(s). Published by Maximum Academic Press, Fayetteville, GA. This article is an open access article distributed under Creative Commons Attribution License (CC BY 4.0), visit https://creativecommons.org/licenses/by/4.0/.